

EVAPORATION HEAT TRANSFER COEFFICIENT IN SINGLE CIRCULAR SMALL TUBES FOR FLOW OF C_3H_8 AND CO_2

Agus S. Pamitran^a, Nasruddin^a, dan Jong-Taek Oh^b

^aDepartment of Mechanical Engineering
University of Indonesia
Kampus Baru UI, Depok (16424)
Indonesia

Phone: +62-21-7270032, FAX: +62-21-7270033, E-mail: pamitran@eng.ui.ac.id

^bDepartment of Refrigeration Engineering
Chonnam National University
South Korea

Abstract

An experimental study of evaporation heat transfer coefficient in single circular small tubes was conducted for flow of C_3H_8 and CO_2 under some various flow conditions. The test matrix encompasses the entire quality range from 0.0 to 1.0, mass fluxes from 50 to 600 $kg\ m^{-2}\ s^{-1}$, heat fluxes from 5 to 70 $kW\ m^{-2}$ and saturation temperatures from 0 to 10°C. The test section was made of circular stainless steel tubes with inner diameters of 3.0 mm and 1.5 mm, and a length of 2000 mm in horizontal orientation. The test section was heated uniformly by applying an electric power to the tubes directly. Effects of mass flux, heat flux, saturation temperature and inner tube diameter on heat transfer coefficient are reported in the present study. Laminar flow was observed in the evaporative small tubes and considered in the modification of boiling heat transfer coefficient and pressure drop correlations.

Keywords: natural refrigerant, C_3H_8 , CO_2 , evaporation, heat transfer coefficient, small tube

1. Introduction

The primary chemicals used as refrigerants, chlorofluorocarbons (CFCs), and the compounds being considered as their replacements (HCHCs) have been intensely studied because of concerns about chlorine chemistry effects on ozone layer. Increasing attention is being given to the potential contributions of these compounds to global warming. In addition, recent awareness of the environmental protection effort and the advantages of process intensification have led to a demand for natural refrigerants evaporation with smaller evaporators for use in the refrigeration, air conditioning and process industries. However, heat transfer for two-phase flows in small tubes cannot be properly predicted using the existing procedures and correlations that are intended to be applied for large tubes with conventional CFCs/HFCs/HFCs refrigerants. C_3H_8 and CO_2 , a long term alternative refrigerants, will be important in the future for compact heat exchanger applications due to their performance, their lack of impact on the environment (zero ODP and low GWP) and their physical properties.

There are relatively few published works that relate

to two-phase flow heat transfer for natural refrigerants in small tubes compared to the amount of data available for conventional refrigerants in large tubes. Compared with conventional tubes, evaporation in a small tube may provide a higher heat transfer coefficient due to its higher contact area per unit volume of fluid. Several studies dealing with two-phase flow heat transfer in small tubes, as reported by Tran et al. (1996), Kandlikar and Steinke (2003) and Zhang et al. (2004), have been published in the past years. However, the published correlations could not predict well the heat transfer coefficient for evaporation in small tubes.

This study was undertaken to obtain experimental data for natural refrigerants and to determine its local heat transfer coefficient during evaporation in small tubes. The effects of mass flux, heat flux, saturation temperature and inner tube diameter on heat transfer coefficient were shown. The heat transfer coefficient of each working refrigerants were compare. The experimental results were compared with several existing heat transfer coefficient correlations. A modified correlation of evaporation heat transfer coefficient for heat exchanger with small tubes design



was developed in this study.

2. Experiments

2.1 Experimental test facility

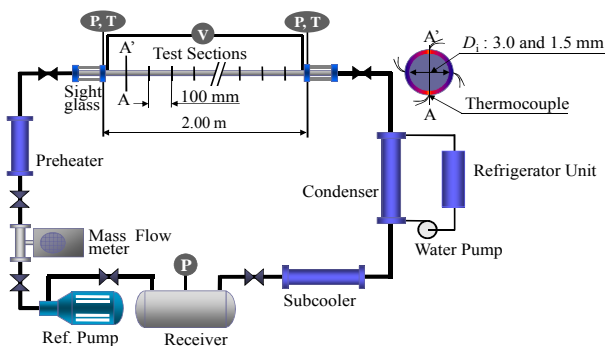


Fig. 1

Table 1 Experimental conditions

Test section	Horizontal stainless-steel circular smooth small tubes
Quality	up to 1.0
Working refrigerant	$\text{C}_3\text{H}_8, \text{CO}_2$
Inner diameter (mm)	3.0 and 1.5
Tube length (mm)	2000
Mass flux ($\text{kg}/(\text{m}^2 \cdot \text{s})$)	50 – 600
Heat flux (kW/m^2)	5 – 70
Inlet T_{sat} ($^{\circ}\text{C}$)	0 – 10

The experimental test facility mainly consists of a refrigerant flow system and test section. Fig. 1 shows a schematic diagram of the experimental facility. As shown in Fig. 1, the refrigerant flow system consists of a condensing unit, a receiver, a refrigerant pump, a mass flow meter and a preheater. Vapor phase refrigerant from the evaporative test section is condensed into liquid phase in the condensing unit. The condensed refrigerant is then supplied to the receiver. The refrigerant is then pumped by the refrigerant pump. The pump is connected to an electric motor controller that is used to control the flow rate of the refrigerant. A Coriolis-type mass flow meter is used to measure the refrigerant flow rate. The mass quality at the inlet of the test section is controlled by installing a preheater.

The test sections are made of circular stainless steel smooth tubes with inner diameters of 3.0 mm and 1.5 mm and a heated length of 2000 mm in horizontal orientation. For evaporation at the test section, a certain electric power is conducted from an electric transformer to the test section. The input electric voltage and current are adjusted in order to control the input power. The test section is well insulated with rubber and foam. The outside tube wall temperatures at the top, both sides, and bottom are measured at 100 mm axial intervals from the

start of the heated length with thermocouples at each measured site. The local saturation pressure, which is used to determine the saturation temperature, is measured using bourdon tube type pressure gauges at the inlet and the outlet of the test section, as shown in Fig. 1. Pressure transducer is installed to measure pressure gradient of the refrigerant flow along the inlet-outlet of the test section. Sight glasses with the same inner diameter as the test section are installed to visualize the flow. Table 1 lists the experimental set-up conditions in this study. The physical properties of the refrigerant are obtained by referencing the REFPROP 8.

2.2 Data reduction

The measured saturation pressure at the inlet and outlet of the test section is used to obtain local physical properties of the refrigerant. The mass quality, x , along the test section is determined based on the local thermodynamic properties.

$$x = \frac{i - i_f}{i_{fg}} \quad (1)$$

where i is enthalpy ($\text{kJ kg}^{-1} \cdot \text{K}^{-1}$), f is saturated liquid condition and g is saturated vapor condition. The subcooled length, z_{sc} , is calculated using the following equation to determine the initial point of saturation.

$$z_{\text{sc}} = L \frac{i_f - i_{fi}}{\Delta i} = L \frac{i_f - i_{fi}}{(Q/W)} \quad (2)$$

where L is tube length (m), i is enthalpy ($\text{kJ kg}^{-1} \cdot \text{K}^{-1}$), f is saturated liquid condition, g is saturated vapor condition, Q is electric power (kW) and W is mass flow rate (kg s^{-1}). The saturation pressure at the initial point of saturation is then determined by interpolating the measured pressure and the subcooled length. The local heat transfer coefficients, h , along the length of the test section are defined as follows:

$$h = \frac{q}{T_{\text{wi}} - T_{\text{sat}}} \quad (3)$$

where q is heat flux (kW/m^2), T is temperature (K), w is wall of test section, i is inner side and sat is saturation condition. The inside tube wall temperature, T_{wi} is the average temperature of the top, both right and left sides, and bottom wall temperatures, and is determined using steady-state one-dimensional radial conduction heat transfer through the test section wall.

3. Result and discussion

Fig. 2 shows the effect of mass flux on heat transfer coefficient. Fig. 2 shows an insignificant effect of mass flux on heat transfer coefficient at low quality region. The insignificant effect of mass flux on heat transfer



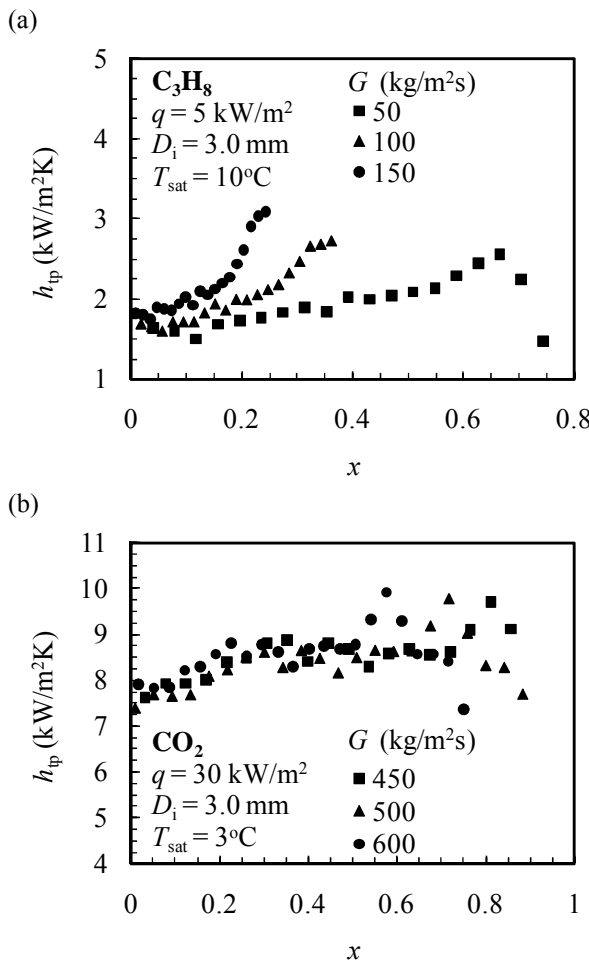


Fig. 2 Effect of mass flux on heat transfer coefficient

coefficient at the low quality region indicates that nucleate boiling heat transfer is predominant. The high nucleate boiling heat transfer is supposed because of the physical properties of the refrigerants and the geometric effect of the small tubes. Several studies with small tubes, including Kew and Cornwell (1997) and Bao et al. (2000), reported that nucleate boiling is predominant in small channels, which is opposite to that of the predominantly convective-dominated heat transfer in conventional channel. Using 1.95 mm tube, Bao et al. (2000) showed that the heat transfer coefficients were independent of mass flux. At the moderate quality region, heat transfer coefficients increase with increasing mass flux and vapor quality. The effect of mass flux on the heat transfer coefficient appears at moderate-high vapor quality, wherein the effect is higher with increasing vapor quality. A higher mass flux results in greater heat transfer coefficient at moderate-high vapor quality due to the increasing convective boiling heat transfer contribution. At the high quality region, the decrease in the heat transfer coefficient occurs at a lower quality under the higher mass flux condition. This trend agrees (a)

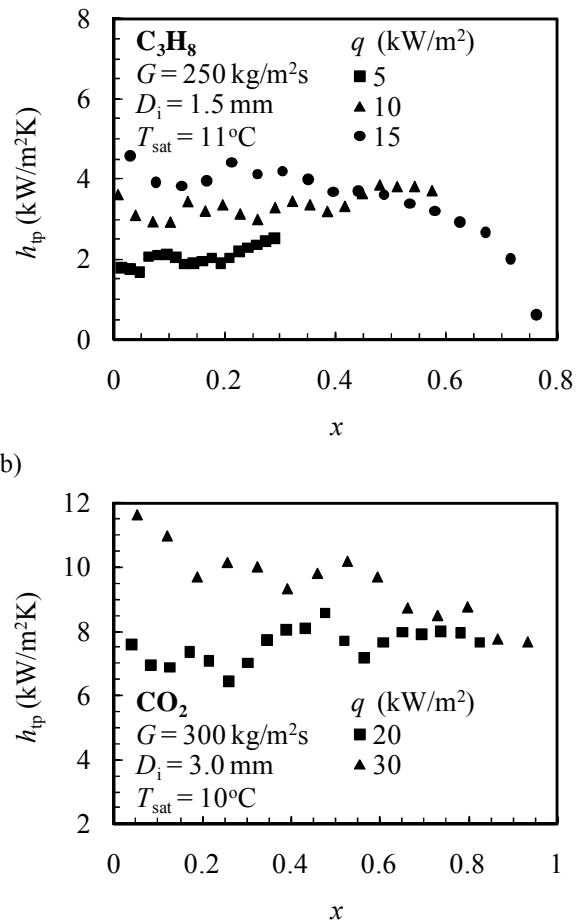


Fig. 3 Effect of heat flux on heat transfer coefficient

with the small tube CO_2 studies of Pettersen (2004) and Yun et al. (2005). For the higher mass flux condition in the convective evaporation region, the increase in the heat transfer coefficient appears at a lower quality, which can be explained by the annular flow becoming dominant with increasing quality. Nucleate boiling suppression appears earlier for the higher mass flux, which means that convective heat transfer appears earlier under the higher mass flux condition. The lower mass flux condition results show smaller increases in the heat transfer coefficient in the convective region. The heat transfer coefficients suddenly increase in the annular flow region before the initial dry-out, which can be explained that as quality is increased in annular flow, the effective wall superheat decreases due to the thinner liquid film or less thermal resistance.

Fig. 3 shows that a strong dependence of the heat transfer coefficients on the heat flux appears at the low quality region for C_3H_8 and CO_2 . At the low quality region, the heat transfer coefficients increased with increasing heat flux. Nucleate boiling is known to be dominant in the initial stage of evaporation, particularly



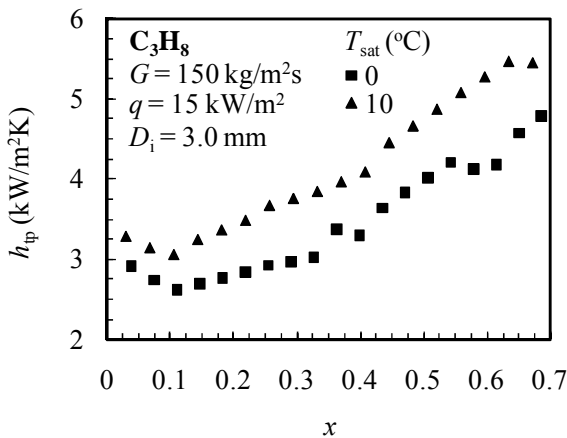


Fig. 4 Effect of saturation temperature on heat transfer coefficient

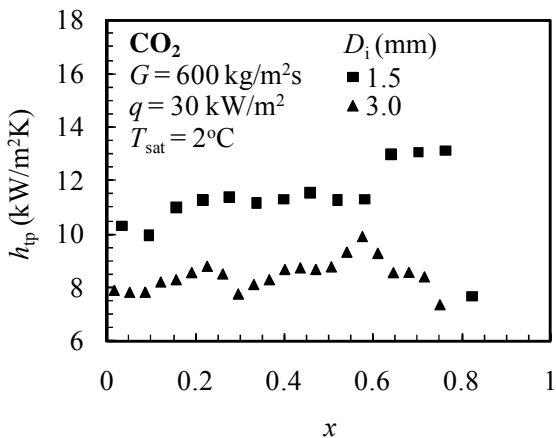


Fig. 5 Effect of inner tube diameter on heat transfer coefficient

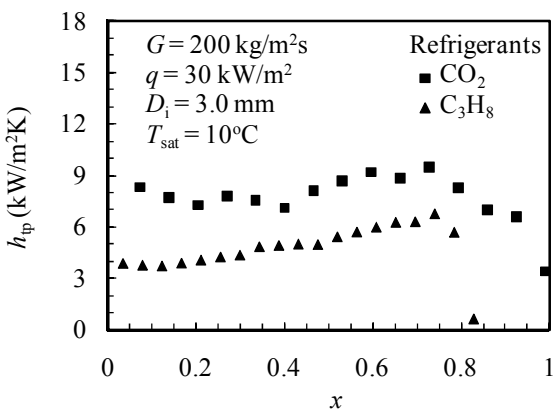


Fig. 6 Comparison of heat transfer coefficient

under high heat flux conditions. The effect of heat flux on the heat transfer coefficient shows the dominance of nucleate boiling heat transfer. Nucleate boiling is suppressed at high quality where the effect of heat flux on heat transfer coefficient becomes lower. As the heat flux increases at high qualities, the evaporation is more

active and the dry-out quality becomes lower. The trend illustrated in Fig. 3 agrees with previous studies, e.g. Kew and Cornwell (1997) and Yan and Lin (1998).

The effect of saturation temperature is depicted in Fig. 4. Heat transfer coefficient increases with an increase in saturation temperature, which is due to a more active nucleate boiling, as shown by the present experimental data. The results can also be explained with the fluid's physical properties such as pressure, density ratio ρ_f/ρ_g , viscosity ratio μ_f/μ_g and surface tension. As shown in Table 2, the higher temperature of 10°C has a higher pressure, lower density ratio ρ_f/ρ_g , lower viscosity ratio μ_f/μ_g and lower surface tension. The vapor formation in boiling process explains that a higher pressure and lower surface tension provides a higher heat transfer coefficient. The working refrigerants have a lower density ratio ρ_f/ρ_g for the higher temperature test condition. Lower density ratio ρ_f/ρ_g causes a lower vapor velocity. Lower vapor velocity then causes a lower suppression of nucleate boiling, which is dominant at lower vapor quality region. Therefore, Fig. 4 depicts that the heat transfer coefficient is higher for the higher saturation temperature test condition at lower vapor quality region. However, at higher vapor quality region the dropping of heat transfer coefficient occurs for the higher saturation temperature test condition. Lower viscosity ratio μ_f/μ_g causes the liquid film is easier for breaking, which is the reason that the dry-out comes easier.

Fig. 5 illustrates the effect of inner tube diameter on heat transfer coefficient. At the low quality region, smaller inner tube diameter shows higher heat transfer coefficient. This is due to a more active nucleate boiling in a smaller diameter tube. As the tube diameter becomes smaller, the contact surface area of the heat transfer increases. The more active nucleate boiling causes dry-patches to appear earlier. The quality for rapid increase in heat transfer coefficient is lower for the smaller tube. It is supposed that the annular flow appears at a lower quality in the smaller tube. The dry-out quality is relatively lower for the smaller tube.

Fig. 6 shows a comparison of heat transfer coefficient of C_3H_8 and CO_2 . The heat transfer coefficient of CO_2 was higher than that of C_3H_8 during evaporation under all test conditions. The higher heat transfer coefficient of CO_2 is believed to be due to its high boiling nucleation. CO_2 has much higher pressure and much lower surface tension than C_3H_8 . Table 2 gives a comparison of the physical properties of C_3H_8 and CO_2 . CO_2 has much lower density ratio ρ_f/ρ_g than C_3H_8 , which causes a lower vapor velocity. A lower vapor velocity causes a lower suppression of nucleate boiling. CO_2 has also much lower viscosity ratio μ_f/μ_g than C_3H_8 , which means that the liquid film of CO_2 is easier for breaking.



Table 2 Physical properties of C₃H₈ and CO₂ at 10 and 0 °C

T (°C)	Refrigerant	P (MPa)	ρ_f (kg/m ³)	ρ_g (kg/m ³)	ρ_f/ρ_g	μ_f (10 ⁻⁶ Pa s)	μ_g (10 ⁻⁶ Pa s)	μ_f/μ_g	σ (10 ⁻³ N/m)
10	C ₃ H ₈	0.636	515	13.8	37.32	113.8	8.15	13.96	8.85
0	CO ₂	4.497	861.7	134.4	6.41	86.37	15.46	5.59	2.77
0	C ₃ H ₈	0.474	529	10.36	51.06	126.2	7.79	16.2	10.13
0	CO ₂	3.481	928.1	97.3	9.54	105.4	14.31	7.37	4.55

The heat transfer coefficients of the present study were analyzed using six previous heat transfer coefficient correlations and compared. Overall, the Shah's (1988) correlation gave the best prediction of all six correlations. Shah's (1988) correlations is developed using a large data with conventional tubes. Gungor and Winterton (1987), Jung et al. (1989), Tran et al. (1996), Wattelet et al. (1994) and Kandlikar and Steinke (2003) provided a quite large deviation on the prediction with an overall mean deviation more than 50%. The correlations of Shah (1988), Gungor and Winterton (1987) and Jung et al. (1989) gave a better prediction for the present CO₂ data, and the correlation of Tran et al. (1996) gave a better prediction for the present C₃H₈ data. The correlations of Wattelet et al. (1994) and Kandlikar and Steinke (2003) fail to predict the heat transfer coefficient for the present experimental data. It shows a necessary to improve the existing correlation with more kind of working fluids and more various test conditions.

4. Development of new correlation

4.1 Modification of F factor

Two important mechanisms of nucleate boiling and forced convective evaporation, mainly govern flow boiling heat transfer. Because of its high boiling nucleation, the appearance of convective heat transfer for evaporative refrigerants in small tubes is delayed compared with that in conventional tubes. Moreover, the working fluid of CO₂ has a high nucleate boiling heat transfer contribution due to its lower surface tension and high pressure. Therefore, the prediction of convective heat transfer contribution for refrigerants in small tubes will be different from that in conventional tubes. The new heat transfer coefficient correlation in this study was developed only with the experimental data obtained prior to dry-out.

Chen (1966) introduced a multiplier factor $F=f_n(X_{it})$ to account for the increase in convective turbulence due to the presence of a vapor phase. Chen (1966) reported the factor, F , to be a function of X_{it} , which needs to be evaluated again physically for flow boiling heat transfer in minichannels which has laminar flow condition due to the small diameter effect. The liquid-vapor flow condition of this experimental result shows 65% turbulent-turbulent, 28% laminar-turbulent, 6% turbulent-laminar and 1% laminar-laminar. By considering the flow conditions (laminar or turbulent) in the Reynolds number factor F , Zhang et al. (2004) introduced a relationship between the Reynolds number factor F and the two-phase frictional multiplier based on pressure gradient for liquid alone flow ϕ_f^2 , $F=f_n(\phi_f^2)$, where ϕ_f^2 is a general form for four conditions according to Chisholm (1967),



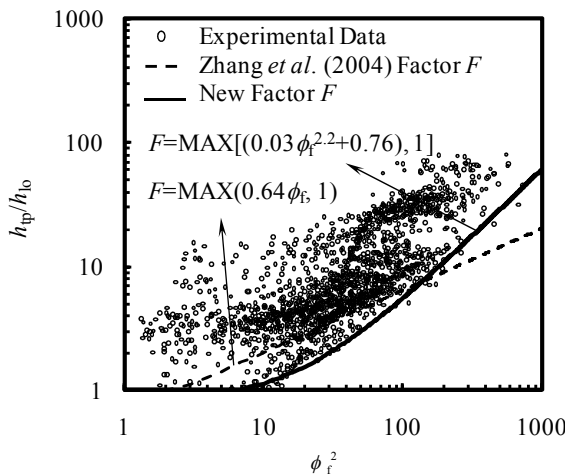


Fig. 7 Modified F factor for convective heat transfer coefficient

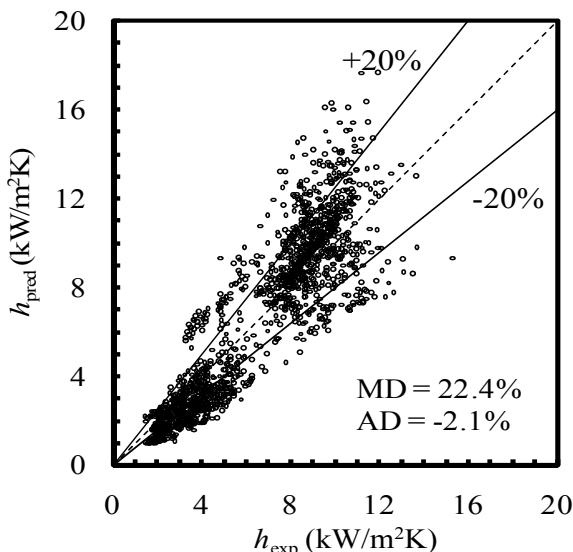


Fig. 8 Heat transfer coefficient comparison between the present experimental data (h_{exp}) and the prediction with the newly modified correlation (h_{pred})

$$\phi_f^2 = 1 + \frac{C}{X} + \frac{1}{X^2} \quad (4)$$

For liquid-vapor flow conditions of turbulent-turbulent (tt), laminar-turbulent (vt), turbulent-laminar (tv), and laminar-laminar (vv), the values of Chisholm parameter C are 20, 12, 10, and 5, respectively. The value of C in this study is found by an interpolation of the Chisholm parameter, C . The Martinelli parameter, X , is defined as follows:

$$X = \left[\left(-\frac{dp}{dz} F \right)_f \Big/ \left(-\frac{dp}{dz} F \right)_g \right]^{1/2} = \left(\frac{f_f}{f_g} \right)^{1/2} \left(\frac{1-x}{x} \right) \left(\frac{\rho_g}{\rho_f} \right)^{1/2} \quad (5)$$

where $(dp/dz F)$ is pressure gradient due to friction (N

$\text{m}^{-2} \text{m}^{-1}$) and ρ is density (kg m^{-3}). The friction factor, f , in Eq. (5) was obtained by considering the flow conditions of laminar-turbulent flows, where $f = 16 \text{Re}^{-1}$ for $\text{Re} < 2300$ (laminar flow) and $f = 0.079 \text{Re}^{-0.25}$ for $\text{Re} > 3000$ (turbulent flow). The laminar-turbulent transition Reynolds number (Re) was referred from Yang and Lin (2007).

The liquid heat transfer is defined by the Dittus-Boelter correlation,

$$h_{\text{lo}} = 0.023 \frac{k_f}{D} \left[\frac{G(1-x)D}{\mu_f} \right]^{0.8} \left(\frac{c_p \mu_f}{k_f} \right)^{0.4} \quad (6)$$

where h is heat transfer coefficient ($\text{kW m}^{-2} \text{K}^{-1}$), k is thermal conductivity ($\text{kW m}^{-1} \text{K}^{-1}$), D is diameter (m), G is mass flux ($\text{kg m}^{-2} \text{s}^{-1}$), x is vapor quality, μ is viscosity ($\text{Pa}\cdot\text{s}$), c_p is specific heat ($\text{kJ kg}^{-1} \text{K}^{-1}$) and lo is liquid only condition.

The factor F is a convective two-phase multiplier that accounts for enhanced convective due to the co-current flow of liquid and vapor. A new factor F as shown in Fig. 7 was developed with a regression method using the present experimental data. The new factor F can be expressed as follows:

$$F = \text{MAX} \left[\left(0.03 (\phi_f^2)^2 + 0.76 \right), 1 \right] \quad (7)$$

4.2 Nucleate boiling contribution

The mass flux is believed to have a significant effect on the suppression of nucleate boiling. A higher mass flux is corresponding to a higher suppression nucleate boiling. For evaporation in a small tube, the suppression is lower than that in a conventional tube. The nucleate boiling heat transfer for the experimental data was predicted using the Cooper (1984) correlation, which is a pool boiling correlation developed based on an extensive study. For a surface roughness of $1.0 \mu\text{m}$, the correlation is given as follows:

$$h = 55 P_r^{0.12} (-0.4343 \ln P_r)^{-0.55} M^{-0.5} q^{0.67} \quad (8)$$

where the heat flux, q , is in W m^{-2} , P_r is the reduced pressure ($P_r = P_{\text{sat}}/P_{\text{crit}}$) and M is Molecular weight (kg kmol^{-1}). Kew and Cornwell (1997), using R-141b in a tube with a length of 500 mm and inner diameters of 1.39–3.69 mm, showed that the Cooper (1984) pool boiling correlation best predicted their experimental data.

Chen (1966) defined the nucleate boiling suppression factor, S , as a ratio of the mean superheat ΔT_e to the wall superheat ΔT_{sat} . The Chen's factor S was developed with a conventional tube hence further evaluation is needed to apply for refrigerants in small tubes. Jung et al. (1989) proposed a convective boiling heat transfer multiplier factor N as a function of the quality, heat flux, and mass flow rate (represented by



using martinelli parameter, X_{tt} , and Boiling number, Bo) to represent the strong effect of nucleate boiling in flow boiling by comparing it with that in nucleate pool boiling, h_{nbc}/h_{pb} . To consider laminar flow in small tubes, the Martinelli parameter, X_{tt} , is replaced by the two-phase frictional multiplier, ϕ_f^2 . Using the experimental data from this study, a new nucleate boiling suppression factor, a ratio of h_{nbc}/h_{pb} , is proposed as follows:

$$S = 1.11(\phi_f^2)^{0.032} Bo^{0.135} \quad (9)$$

5. Concluding remarks

Mass flux and vapor quality have an insignificant effect on the heat transfer coefficient at the low quality region. At the moderate quality region, the heat transfer coefficient increase with mass flux and vapor quality. At the high quality region, a decrease in the heat transfer coefficient occurs at a lower quality for a higher mass flux condition. A strong dependence of the heat transfer coefficients on the heat flux appears at the low quality region. The Shah's (1988) correlation gave the best prediction among the six reported correlations.

The physical properties of the refrigerant and geometric effect of the small tube must be considered when developing a new heat transfer coefficient correlation. Laminar flow appears during flow boiling in small channels. Therefore, in this study, a modified correlation of the multiplier factor on the convective boiling contribution, F , and the nucleate boiling suppression factor, S , was developed using a laminar flow consideration. A modified boiling heat transfer coefficient correlation based on the superposition model for refrigerants in small tubes showed a mean deviation (MD) and average deviation (AD) of 22.4% and -2.1%, respectively.

References

[1] Bao, Z.Y., Fletcher, D.F. and Haynes, B.S., 2000. Flow boiling heat transfer of freon R11 and HCFC123 in narrow passages. *Int. J. Heat Mass Transfer* 43, 3347–3358.

[2] Chen, J.C., 1966. A correlation for boiling heat transfer to saturated fluids in convective flow. *Ind. Eng. Chem. Process Des. Dev.* 5, 322–329.

[3] Chisholm, D., 1967. A theoretical basis for the Lockhart–Martinelli correlation for two-phase flow. *Int. J. Heat Mass Transfer* 10, 1767–1778.

[4] Cooper, M.G., 1984. Heat flow rates in saturated nucleate pool boiling – a wide-ranging examination using reduced properties. *Advances in Heat Transfer* 16, 157–239 (Academic Press).

[5] Gungor, K.E. and Winterton, H.S., 1987. Simplified general correlation for saturated flow boiling and comparisons of correlations with data. *Chem. Eng. Res.* 65, 148–156.

[6] Jung, D.S., McLinden, M., Radermacher, R. and Didion, D., 1989. A study of flow boiling heat transfer with refrigerant mixtures. *Int. J. Heat Mass Transfer* 32 (9), 1751–1764.

[7] Kandlikar, S.G. and Steinke, M.E., 2003. Predicting heat transfer during flow boiling in minichannels and microchannels. *ASHRAE Trans.* CH-03-13-1, 667–676.

[8] Kew, P.A. and Cornwell, K., 1997. Correlations for the prediction of boiling heat transfer in small-diameter channels. *Appl. Therm. Eng.* 17 (8–10), 705–715.

[9] Pettersen, J., 2004. Flow vaporization of CO₂ in microchannels tubes. *Exp. Therm. Fluid Sci.* 28, 111–121.

[10] Shah, M.M., 1988. Chart correlation for saturated boiling heat transfer: equations and further study. *ASHRAE Trans.* 2673, 185–196.

[11] Tran, T.N., Wambganss M.W. and France, D.M., 1996. Small circular- and rectangular-channel boiling with two refrigerants. *Int. J. Multiphase Flow* 22 (3), 485–498.

[12] Wattelet, J.P., Chato, J.C., Souza, A.L. and Christoffersen, B.R., 1994. Evaporative characteristics of R-12, R-134a, and a mixture at low mass fluxes. *ASHRAE Trans.* 94-2-1, 603–615.

[13] Yan, Y.Y. and Lin, T.F., 1998. Evaporation heat transfer and pressure drop of refrigerant R-134a in a small pipe. *Int. J. Heat Mass Transfer* 41, 4183–4194.

[14] Yang, C.Y. and Lin, T.Y., 2007. Heat transfer characteristics of water flow in microtubes. *Exp. Thermal and Fluid Sciences* 32, 432–439.

[15] Zhang, W., Hibiki, T. and Mishima, K., 2004. Correlation for flow boiling heat transfer in mini-channels. *Int. J. Heat Mass Transfer* 47, 5749–5763.



